2010

Development of a compact optical system for a forward-looking endoscope

Anandi Kalyan Dutta
Louisiana State University and Agricultural and Mechanical College

DEVELOPMENT OF A COMPACT OPTICAL SYSTEM FOR A FORWARD-LOOKING ENDOSCOPE

A

Thesis

Submitted to the Graduate Faculty of the
Louisiana State University and
Agricultural and Mechanical College
in partial fulfillment of the
requirements for the degree of
Master of Science in Electrical Engineering

in

The Department of Electrical and Computer Engineering

by

Anandi Kalyan Dutta
B.S., American International University-Bangladesh, 2006
December 2010

ACKNOWLEDGMENTS

I would like to express my deep gratitude to my supervisor, Dr. Martin Feldman for his intense guidance throughout my whole graduate studies. Moreover, I want to thank Dr. Pratul K. Ajmera and Dr. Dooyoung Hah for serving on the thesis committee and for their sincere time, concern and guidance. I also want to thank Ragavendra Shankar Murthi for doing the hard work of sanding down the sample chips. I am also thankful to Precious Cantu for her contribution in the optical arrangement system and for permission to use one of her photographs. I am also grateful to Dan Zhang, Daniel J Hebert, M Pallavi Rao, Pradeep Pai and Anirban Sarkar for helping me by sharing their advice and experience.

Also thanks to all my friends and family members for their strong encouragement and care. Then I want to express my deep gratitude to my parents Swapan Dutta and Krishna Debnath, my sister Indira Kalyan Dutta, for their moral support and unconditional love. And special thanks to my husband Subasish Das for his patience, understanding and invaluable friendship.

TABLE OF CONTENTS

ABSTRACT

Optical Coherence Tomography has been effectively used for endoscopy in many previous studies. In this work, a 2 mm diameter forward-looking endoscope is developed with the help of MEMS technology and Optical Coherence Technology (OCT) to obtain in-vivo cross-sectional images of tissues or body cavities. The design consists of a GRIN lens, optical fiber and MEMS chip that are placed in line to fulfill the aim of achieving a 2 mm diameter probe. A standard assembly process has been established for the probe. An anisotropic etching was performed on the sample chip to create the V-groove for carrying the fiber properly. Furthermore, the sample chip was thinned at right thickness to fit in the 2 mm diameter stainless steel tube. Moreover, the optics relating the fiber and the GRIN lens has been tested. The light was transmitted through the core of the fiber and reflected back from the mirror of the GRIN lens. The reflecting angle of the rays was correct to hit the scanning mirror.

CHAPTER 1

INTRODUCTION

In this project, a small structured forward-looking endoscope is developed with the help of MEMS technology and Optical Coherence Technology (OCT) to obtain in-vivo cross-sectional images of tissues or body cavities. Optical Coherence Tomography has been effectively used for endoscopy in many previous studies. The MEMS chip provides the scanning mechanism of the device. The design consists of a GRIN lens, optical fiber and MEMS chip that are placed in line to fulfill the aim of achieving a 1 mm diameter probe. But, in the laboratory, a 2 mm diameter of probe is being assembled. The novel approach of this project ensures high image quality, simplified construction and minimized probe diameter. This endoscope will be used for Cancer treatment and diagnostics.

1.1Definitions

- Optical Coherence Tomography: Optical Coherence Tomography (OCT) is an imaging technique that uses reflected light to obtain cross-sectional images of tissue [1]. Generally the resolution of 5-20 μm and the penetration depth of 1-2 mm have been reported for OCT. OCT has substantial potential in analyzing microstructure of tissues and pathological diagnosis.

- MEMS: MEMS is short for Microelectromechanical Systems. MEMS embraces a wide range of applications including communication systems, biomedical engineering, sensors, actuators, projection displays etc. In this project, a MEMS chip

is developed to carry the micro-scanner mirror.

- Micro-scanner mirror: As the OCT system is built upon creating an image of reflective rays, the system requires a movable micro-scanner mirror. This mirror receives rays and reflects the rays back for a certain angle and range.

- GRIN lens: GRIN (GRadient INdex) lenses gradually vary the index of refraction with the radius of the lens and guide the light rays towards a focus [2].

- Optical Fiber: Optical Fiber is used in this research to guide the light rays with minimal loss. The working principle of optical fiber is based on the total internal reflection.

- Light Source: This research project requires the use of infra-red laser (wavelength = 1.3 μm) as the light source because the longer wavelength of light can penetrate deeper into the tissues for imaging. But for the ease of experiments, visible laser light (0.633 μm) is used as the source.

1.2 Background

1.2.1 Dimensionality

Body tissues and cavities require small-dimension device for diagnosis. OCT has been used to diagnosis the pancreatic-biliary structures through imaging. Therefore, miniaturization of the probe would increase the clinical utility for application in thickened

structures, especially for pediatric applications. As far as reported endoscopes, only one is in a range of 1-2 mm diameter. Cal Tech reported a structure of 1 mm diameter probe. But it suffers problems related to a long flexible shaft and also it has inherent vibration and lifetime problems for its counter rotation mechanism [3].

1.2.2 Side-looking probe vs. Forward-looking probe

In general, the probe mechanism can be divided into two methods: Forward-looking probes and Side-looking probes. Side-looking probes generate images of tissues along the side which is not always helpful. On the other hand, forward-looking probes produce images of tissue ahead of where the probe is placed. This permits guiding the path for the viewers, so that the probe does not damage sensitive areas of the tissue. To form the image, the side-looking probes need one pass through the lens. Hence, the optics principle is simpler than the forward-looking probes and the diameter is smaller. On the other hand, conventional forward-looking probes require an additional pass alongside the lens. So, they require larger diameters than the side-looking probes.

1.2.3 Introducing MEMS

There are other techniques for scanning mirrors besides MEMS. Proximal scanning with relay lenses and scanning a mirror with an internal galvanometric motor have been practiced before introducing MEMS. But, MEMS can provide reliable high speed micro-scanners with negligible mechanical vibration and compact packaging compared to other techniques. Thus, MEMS technology has been introduced to the endoscope design. Mostly

electrostatic actuators [5-8] and electro-thermal actuators [9] are used in endoscopes. In this project a scratch drive actuator (SDA) has been used.

CHAPTER 2

COMPONENT DESCRIPTION

2.1 GRIN Lens

The GRIN lens is a significant part of this device. A conventional lens bends light only at its surface when it undergoes a change of refractive index. The shape and smoothness of the surface have to be controlled carefully to focus the rays for forming an image. The GRIN lens bends light within the lens material because of its varying refractive index property. This property effectively guides the rays towards the point of focus smoothly and continually to form an image. This property also minimizes the need for tightly controlled surface curvature of a conventional lens. Therefore, for an endoscopic application, the GRIN lens can efficiently relay an image and couple with an optical fiber compared to conventional lens [10]. Also, the GRIN lens provides small diameter compared to conventional lens. Another important point is that the stable cylindrical shape is very much convenient to fit in the endoscope structure and for mounting with the optical fiber.

By varying the lens length, a flexibility of the focal length and working distance can be achieved. In this project, a 2 mm diameter lens is used and the length of the lens is 2.635 mm. The light rays pass through the lens as sinusoidal waves. The pitch of the lens is chosen based on the length of the sine wave. The length of the GRIN lens is designed correspond to the number of oscillations of the sine wave. If a ray is going through the full period, π, of a lens, then it will make a complete oscillation of a sine wave. In this project, the length of $\pi/8$ lens is chosen. That means the rays will make a oscillation of one-eighth of a sine wave. We bought our lens from NSG America Company and according to their specification the

pitch of the 2 mm diameter lens is 0.125, of 1/8 of a full period.

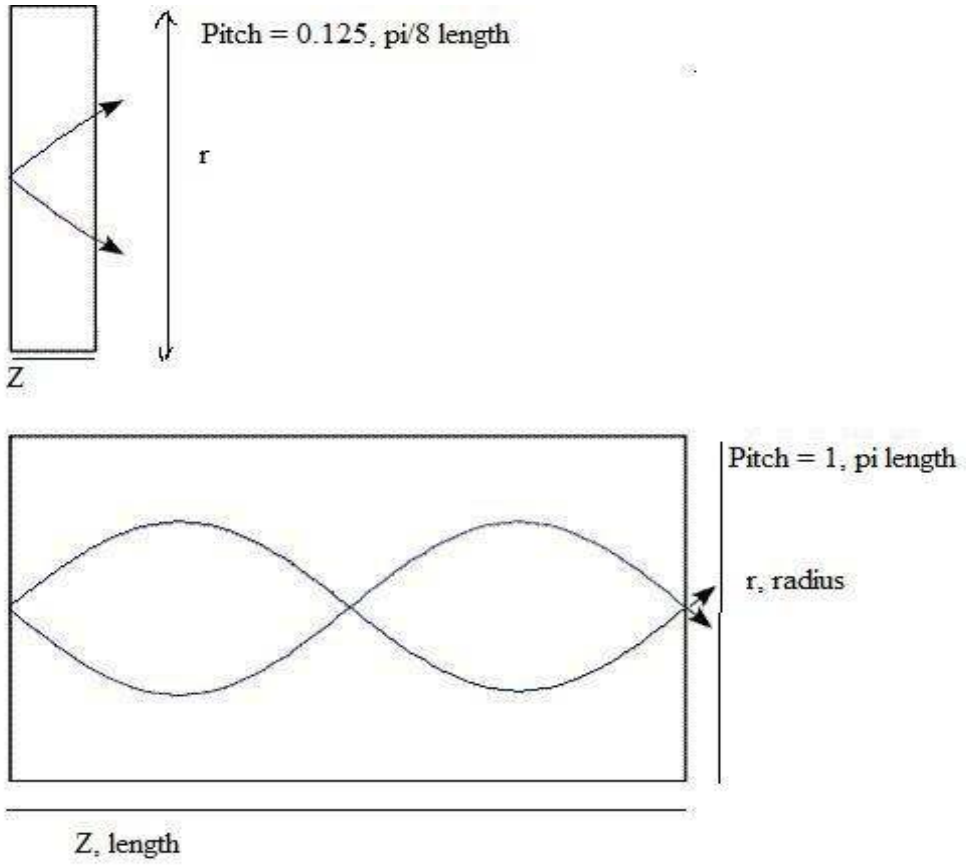

Figure 2.1: Comparison of different pitches in GRIN lens

Figure 2.1 illustrates the concept of different values of pitch. The length of the lens in the bottom figure is one period, so that the rays make a complete sine wave while going through the lens. The pitch of top lens is 0.125, indicating that the light rays make an oscillation of one-eighth of a sine wave.

In a GRIN lens, the refractive index decreases with distance from the axis. The relation between

the refractive index (n) and the radius (r) of the 2 mm diameter lens is shown here:

$$N(r) = N_o (1- \sqrt{A}/ 2*r^{1/2}) \qquad (1)\ [10]$$

N_o = on-axis refractive index of GRIN lens

$\sqrt{A}$= index gradient constant (mm^{-1})

r = radius of lens

For 2 mm diameter lens, $N(r) = 1.643 (1- 0.2958/ 2* r^{1/2})$

The characterization of optical performance can be determined with equation (1). The convergence of light rays for any particular wavelength depends on the index gradient constant. Also, different dispersion relations apply for different lens diameters.

The relation between the lens length (Z) and lens pitch (P) is shown below:

$$2\pi P=\sqrt{A}Z \qquad (2)\ [10]$$

So, how and where the image is formed can be traced by choosing the pitch appropriately. When the GRIN lens is used for imaging purpose, resolution is the most important factor to maintain. Hence, the lens is designed in such a way that it consistently exhibits good image quality despite variation in lens length and index gradient constant.

2.2 MEMS Chip

The MEMS chip is composed of the scanning mirror, SDA actuator and mechanical assembly components. The placement of the MEMS chip is parallel to the optical axis and to match the Optical system, the scanning mirror can be folded up to 74 degrees out-of-plane. This

arrangement has two important advantages over placing the MEMS chip perpendicular to the axis with an in-plane mirror. The alignment tolerance is flexible and the scanning mirror can be fine-tuned with the rest of the optical system after the assembling of the GRIN lens-fibre part. Moreover, the packaging process is more convenient, because the electrical wires can be attached at the front surface of the MEMS chip [11, 13].

The folding mechanism that is associated with scratch drive actuators (SDA) has been chosen for this project because it is better in three aspects than other mechanisms. The advantages are: a) a large folding angle b) precise angle control c) post-fine tuning ability. SDA is an inchworm-like electrostatic actuator. The level of the voltage pulse and the geometry determine its step-size for forward moving. In this chip, the scanning mirror pivots on hinges and is rotated upwards by the SDAs. Thereafter, the spring latches maintain its steady-state angular position. The typical speed of SDA is 1 cm/s corresponding to a mirror scanning frequency of about 180 Hz for a 14° mirror range of rotation [11,13].

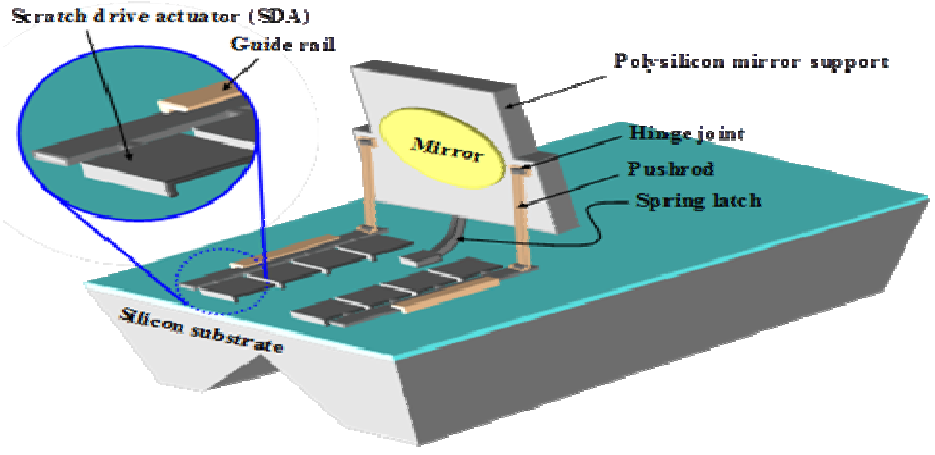

Figure 2.2.1: The scanning micromirror with SDAs (Hah et al)

In Figure 2.2.1, the MEMS chip is shown. This chip is designed by Dr. Dooyoung Hah and the design is sent to the commercial foundry service, Multi-User-MEMS-Processes (MUMPs) [12]. MUMPs would supply two structural polysilicon layers, which will be utilized for all the moving parts, two sacrificial oxide layers for device release, and a metal layer, which is useful for a reflecting surface and bonding pads.

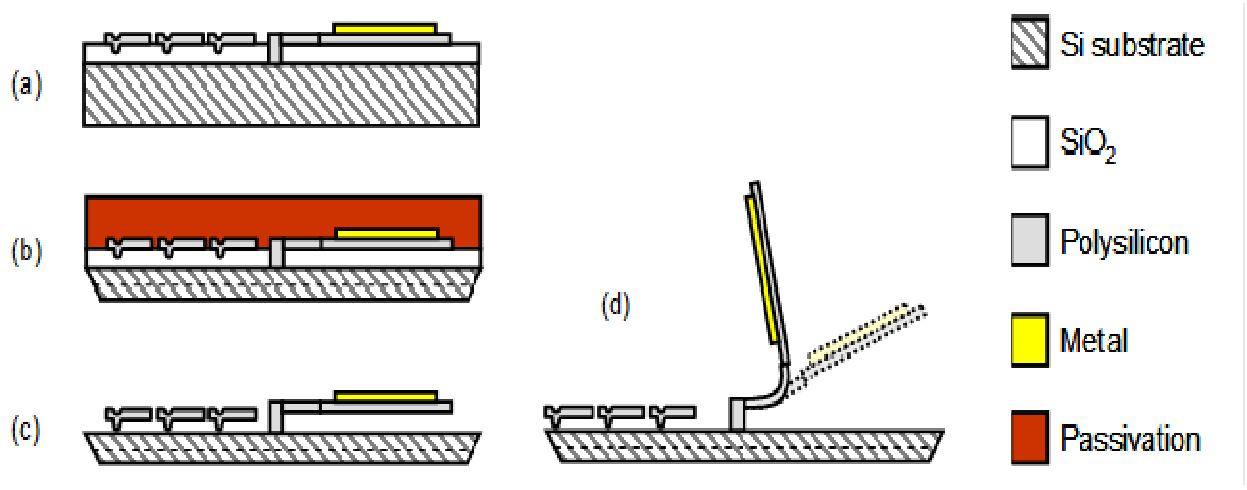

Figure 2.2.2: Fabrication process flow of the MEMS chip (Hah et al)

In Figure 2.2.2, the fabrication process flow of the MEMS chip is described. At first in (a), The basic structure of the MEMS chip without the releasing of the mirror and anisotropic etching is shown. This is how the chip arrives from MUMPs. The chip will be attached with the lens and it will carry the optical fiber also. The whole structure will be placed in a 2 mm inside diameter stainless steel tube. Therefore, the chip needs to be thinned down to fit in the stainless steel tube. In addition, an anisotropic etching will be done to create a V-groove on the

bottom side through which the optical fiber will pass. In step (b), the chip is shown after anisotropic etching and substrate thinning. Thereafter, the moving parts of the chip will be released by etching a sacrificial oxide layer in HF. Step (c) represents the structure of the chip after the mirror release. In the packaging part, thin contact wires will be attached to the bonding pads. Finally, the scanning mirror will be folded up by applying voltage pulse to the SDA. In part (d), the assembly of the scanning mirror with SDAs is shown. The Figure 2.2.2 is not drawn to scale and the hinge joints and pushrod parts are not shown for clarity.

To summarize, the front-side of the MEMS chip includes the scanning mirror, mechanical assembly components and the SDA. The bottom-side of the MEMS chip will be thinned to fit in the stainless steel tube. Moreover, anisotropic etching with KOH (potassium hydroxide) or TMAH (tetramethylammonium hydroxide) will be applied to the bottom of the chip to produce the V-groove to carry the fiber. As the folding up of scanning mirror is the last part of the process, it can be aligned to the optical system. Therefore, the SDA MEMS chip is an effective choice for an in-line optical system.

CHAPTER 3

The Optical Design of the Probe

The resolution and the depth of focus are the two most important considerations for any optical system. That can be determined by the wavelength of the operation and its numerical aperture (NA):

$$\text{Spot size} \approx \frac{\text{wavelength}}{2NA}; \quad \text{Depth of focus} \approx \frac{\text{wavelength}}{2NA^2}$$

The application of the endoscope requires the wavelength of 1.3 μm for maximum tissue penetration. Hence, the choice of wavelength is fixed. But, by ray tracing we can determine the numerical aperture (NA). Again it should be considered that there is a trade-off. By analyzing the equations it can be stated that larger NA can produce better resolution but smaller depth of focus. On the other hand, the axial scan range can be extended by reducing the NA. The maximum NA that can be accommodated by this system is 0.12. This choice is made by considering the NA of the optical fiber. The NA of the fiber is 0.12 for the 0.633 μm He-Ne laser source. The future testing of the endoscope will be done at the University of Arizona. Their system is based on NA of 0.12. Therefore, to accommodate their system, the NA is chosen as 0.12 for this project. A table is presented below for the comparison of NA:

Table 3.1. The design window for spot size and depth of focus (wavelength= 1.3 μm)

NA	0.03	0.045	0.08	0.12
Spot Size, μm	22	14	8.1	5.4
Depth of Focus, μm	720	320	102	45

But, for the ease of experiment, 0.633 μm wavelength (He-Ne laser) is chosen for this thesis. A table is presented below for the comparison of NA for 0.633 μm wavelength.

Table 3.2: The design window for spot size and depth of focus (wavelength= 0.633 μm)

NA	0.03	0.045	0.08	0.12
Spot Size, μm	10.55	7	3.96	2.6
Depth of Focus, μm	351	156	49	21

By comparing table 3.1 and 3.2, we can say that the desired long depth of focus can be achieved with the 1.3 μm wavelength source. In optical coherence tomography, depth of focus determines the scanning range. Hence, the system prefers long depth of focus to achieve large scanning range.

In a GRIN lens, the light rays are bent when they pass through the lens body. In Figure 3.1.1, it is shown how a point source at one end of the lens is transformed into a parallel beam at the other end.

In Figure 3.1.1, two cases are shown where NA is 0.12. The top two traces (red) start at a height of 0.8 mm, and the bottom two traces (green) start at the center of the lens. Both pairs of rays reach the end of the lens at ± 0.268 mm. The rays in each beam exit the lens parallel to each other.

The ray tracing for object point, lens and image point is shown in Figure 3.1.2. The conjugate

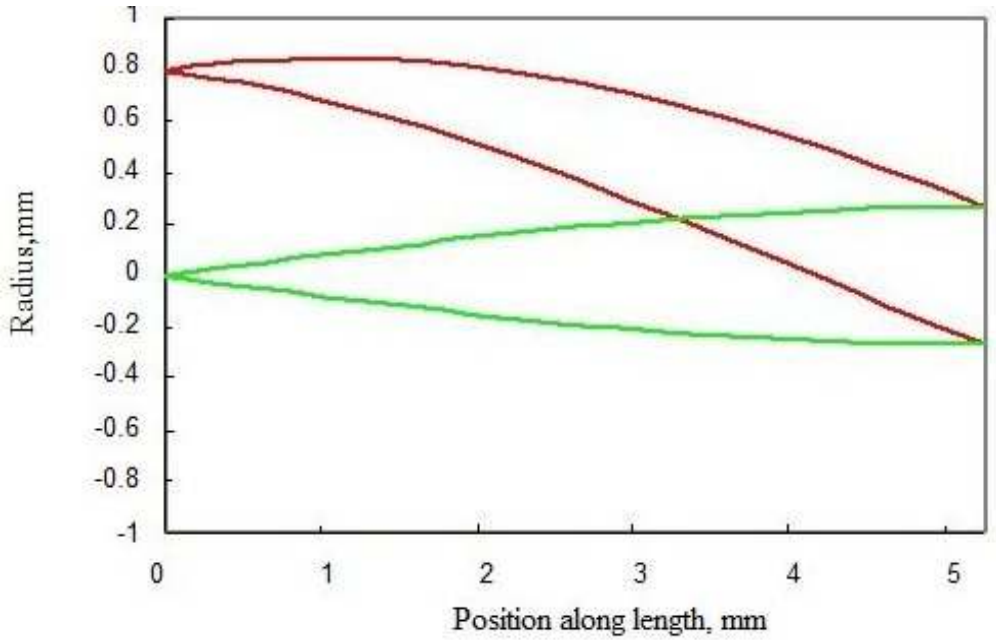

Figure 3.1.1: Ray trace through a GRIN lens of π/4 long and the diameter is 2 mm

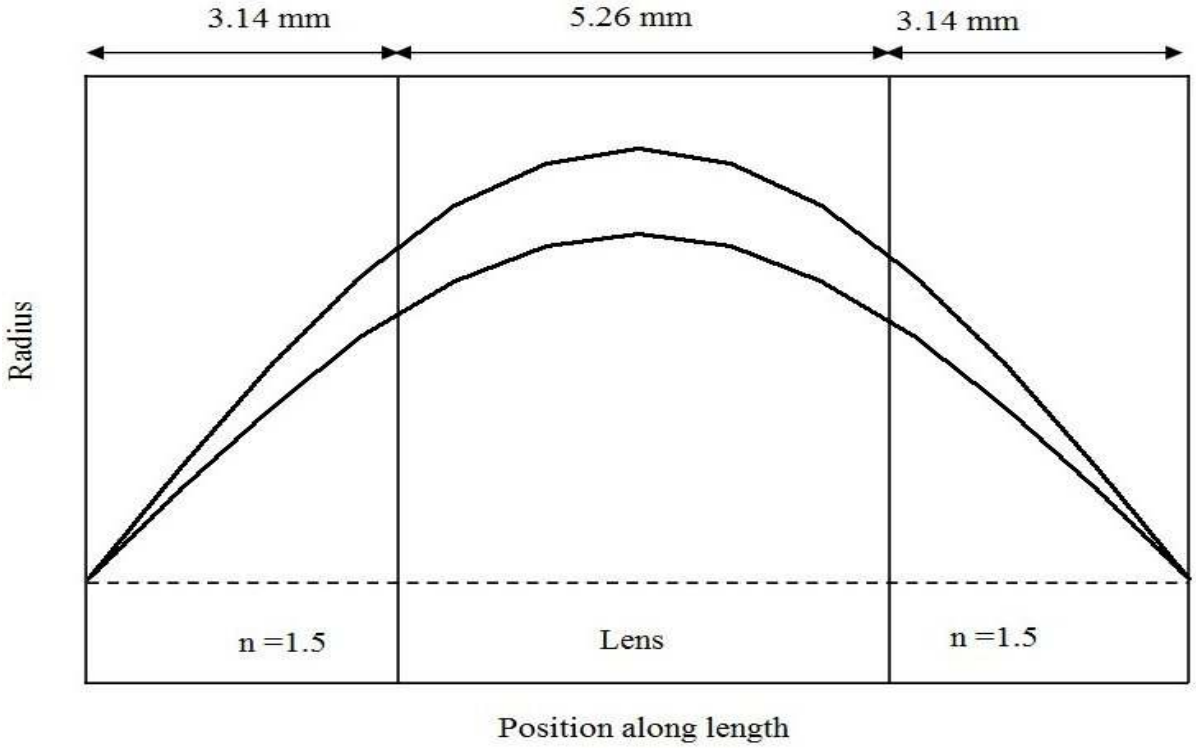

Figure 3.1.2: An example of 1:1 imaging obtained with a π/4 lens.

points are located outside the lens in a material whose index of refraction is 1.5. The image point and object point are spaced at 3.14 mm from lens in opposite directions. Light rays pass in sinusoidal forms inside the lens and they are parallel at the mid-point ($\pi/8$). But, the light rays symmetrically converge to the source point and object point.

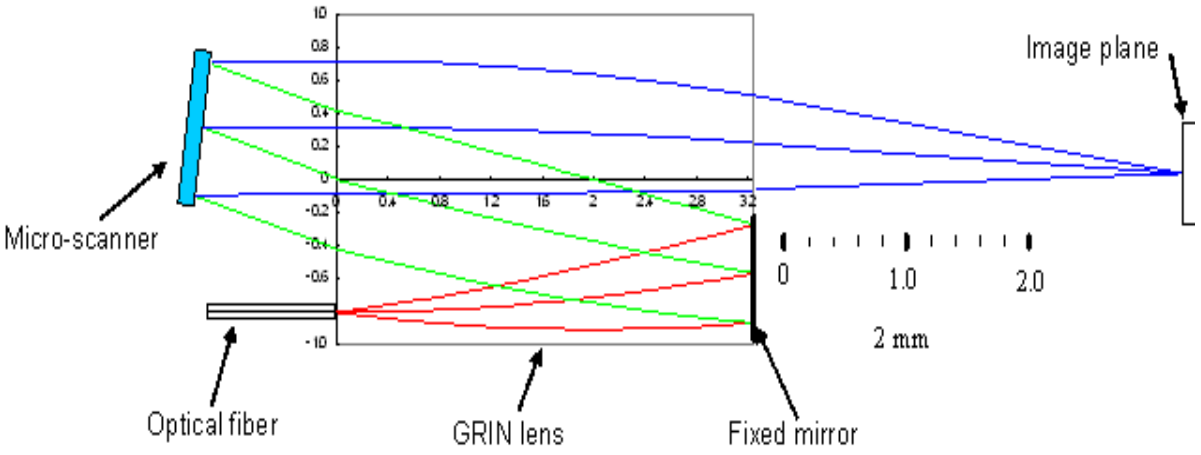

Figure 3.1.3: Path of the light beam from the fiber, lower left, back and forth through the GRIN lens.

By combining segments of the ray tracing in Figures 3.1.1 and 3.1.2, a compact imaging system can be developed. The light is finally brought to a focus 3.14 mm to the right of the lens. The Figure 3.1.3 illustrates a NA of 0.12. For clarity the angular deflection of the micro-scanner has been exaggerated. The Figure 3.1.3 shows the light path for the lens of length $\pi/8$ (2.63 mm) and the diameter of the lens is 2 mm. The light rays pass through the lens and then are reflected back by the Al mirror (fixed mirror in the Figure 3.1.3). Then the reflective light rays exit the lens, strike the scanning mirror, and pass through the lens again. The light rays converge and finally cross the right side of the lens and form an image. The Figure 3.1.2 can be recalled here to

explain the converging principle. Also Figure 3.1.1 can be recalled to understand the total path of rays. As the light passes the first two times through the lens, it completes a $\pi/4$ path. This $\pi/4$ path is equivalent to the sinusoidal path of the Figure 3.1.1. After reflecting from the scanning mirror the light reenters the lens, still as a parallel beam, but at an angle dependent upon the angle of the mirror. It then leaves the lens and is brought to a focus.

The light both passes through and is reflected by the right end of the lens. Therefore, some of the part of the right end of the lens works as a reflecting mirror. The chip will carry the fiber and then the fiber will be attached to the lens by 60 minutes epoxy. The spacing material will be attached to the GRIN lens at the other side. The UV curing optical cement will be used as a spacing material/ spacer. The refractive index of the spacer should be optically matched with the fiber and the lens. It is required that the light reflected from the scanning mirror does not intersect either the mirrored portion of the right surface of the lens, the side of the lens, or the side of the spacer. This depends on the angular range of the scanning mirror. The largest usable angular range for the scanning mirror (at an NA of 0.12) is about 14 degrees. The associated scan of the focused spot is about 1.5 mm long, ¾ of the diameter of the optical aperture, and extends almost to the edge of the spacer [11,13].

The complete arrangement of the lens, fiber and chip is sketched in Figure 3.1.5. The assembly process and the expected results will be discussed in the next chapters. Two types of probe structure are shown In Figure 3.1.6: sharp probes and blunt probes. In the sharp probe configuration, the spacing material is polished and cut into an angle of 45 degrees. The sharp probes are made to use within tissue. The material that is in optical contact with the probe should have at least the refractive index of 1.33 (refractive index of water). The focal plane

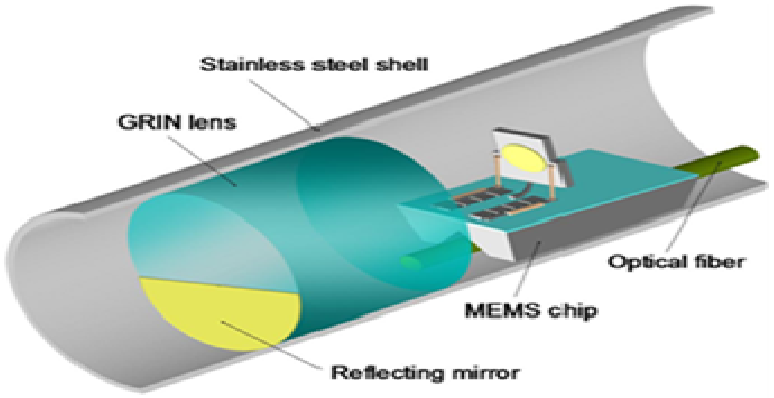

Figure 3.1.5 Sketch of the endoscopic probe. For clarity, the spacing material and electrical wires are not shown here (Feldman et al)

will lie near the sharp edge of the probe. Also, the probe is able to produce the image of half mm into the tissue or body fluid. The oblique nature of the surface of the probe can cause some change in incident angle (8 degree) and focal plane (tilts the focal plane at most 80 μm). But the changes can be compensated if required. For the blunt probe mechanism, the spacing

Figure 3.1.6. Cross section view of (a) blunt and (b) sharp endoscopic probes. (Feldman et al)

material is polished but cut at 90 degrees. The blunt probes are used for imaging into body cavities [11]. Different working distances can be achieved by varying the length of the spacer.

Figure 3.1.7 illustrates the possibility of varying the working distace.

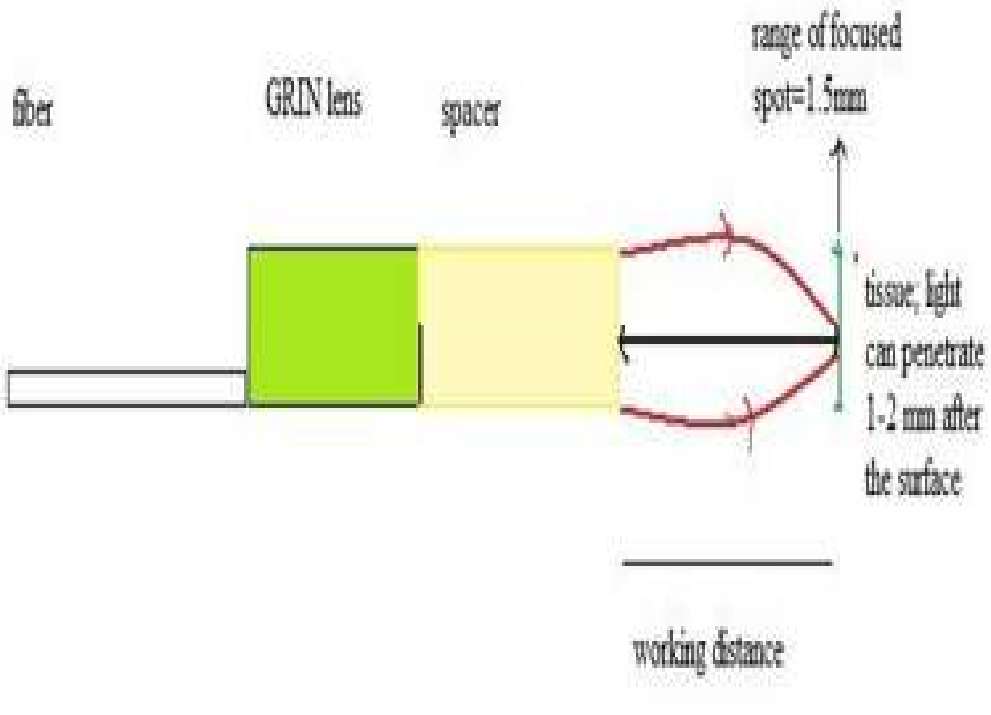

Figure 3.1.7: Working distance variation

CHAPTER 4

FABRICATION AND ASSEMBLY

4.1 Preparing the GRIN Lens

Initial experiments were performed with the 2 mm diameter GRIN lens instead of the 1 mm diameter lens. The goal is to establish a standard procedure of assembling the probe with the 2 mm diameter set-up. Then this procedure will be applied to the 1 mm diameter probe. The feasibility and effectiveness of this process will guide the project for the next step.

One side of the GRIN lens contains the reflecting mirror, and is coated with Aluminium (Al). The physical vapor deposition (PVD) process is followed for depositing Al. The thickness of the Al is 200 nm. This mirror plays an important role in the whole reflection process. Under the microscope, the upper half of the lens was covered with Al foil and scotch tape to prevent deposition. Then the sample was placed on the sample holder of the thermal evaporator. After the end of the evaporation process, Al is coated as a mirror on the bottom half part of the GRIN lens. The GRIN lens coated with Al is shown in Figure 4.1.

4.2 Preparing the MEMS Chip

The design of the MEMS chip was sent to MUMPS (MEMS fab line) [12]. But, in this stage of the project, a 1920 μm by 1920 μm square sample chip was used in the assembling process. Sample chips were fabricated in-house to test the assembling process and optical arrangement. The sample chips were devoid of the scanning mirror and the SDA actuator. However, a V-groove was created with KOH directional etching to carry the optical fiber properly. In addition, the chip was thinned to fit in the stainless steel tube.

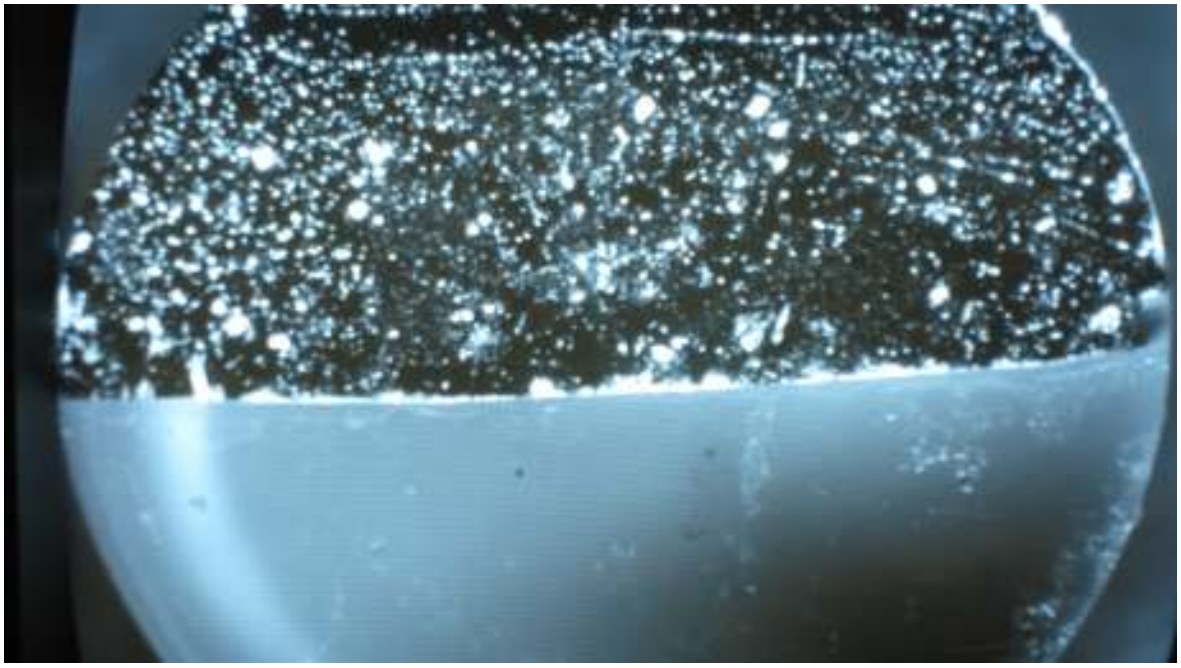

Figure: 4.1 The GRIN lens with the top half coated with aluminum. The image was taken under dark field illumination.

The KOH etching was performed by Dan Zhang and Pradeep Pai. In Figure 4.2.1, the mask opening is W, the height of the V-groove is H and the angle is 54.7 degrees. The KOH

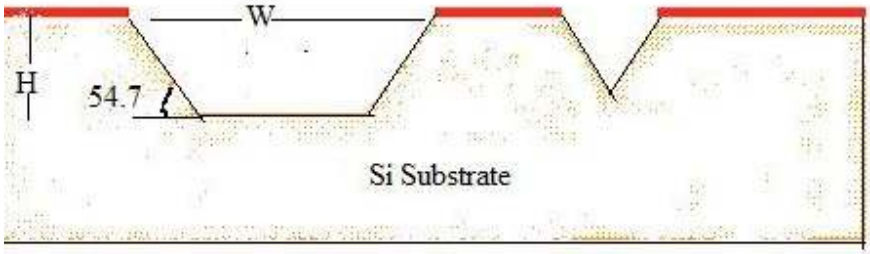

Figure 4.2.1: KOH Anisotropic Etching on Silicon

solution etches the (100) plane and leaves the (111) plane. The mask opening is determined by

considering the required H and angle. The first step was to design a mask with required W and length of the chip. Then the wafer was coated with AZ 9260 photoresist. After the coating, the photoresist was soft baked (at 90^{o}C, 5 minutes on hot plate). The process of lithography, developing resist and hard baking (at 150 ^{o}C, 1 hour in oven) were performed then. The Si_3N_4 was etched by RIE (Reactive Ion Etching) with CF_4. Afterwards, HF etching was done to etch the SiO_2. The hard baked photoresist was removed by RIE with O_2 .Then a 30-35 % KOH solution was applied to etch the Si. In figure 4.2.2, the layers of material are shown.

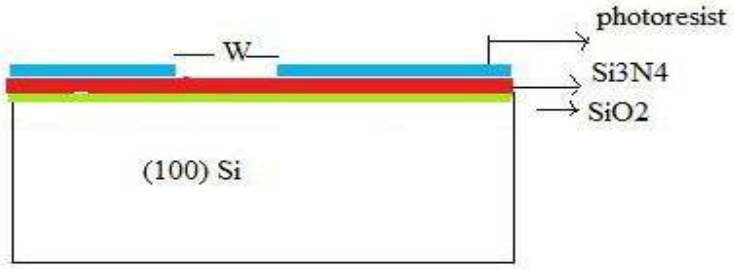

Figure 4.2.2: The layers of material for the KOH etching process

If the original V-groove height is maintained for the assembling process, then the height of the groove will be large for the fiber to fit properly, and the chip will not fit into the 2 mm diameter tube for its thickness. The fiber must touch the edge of the groove for proper optical alignment. The fiber must protrude so it can be pushed into the bottom of the groove. Therefore, to fit the fiber into the groove in exact position, a sanding procedure was done. In Figure 4.2.4, the position of fiber is shown after the thinning process. By considering all the requirements, a range of height is chosen for the groove. The range of sanding down the chip is 142 µm to 263 µm. But it is preferable if the number is close to 142 µm. If the chip thickness is sanded down by 142 µm, it still contains the V-groove. On the other hand, the height of the V-groove would be too small if the chip is sanded down by 263 µm. Hence, the V-groove cannot carry the fiber properly. In

Figure 4.2.3, the original height of the V-groove is shown.

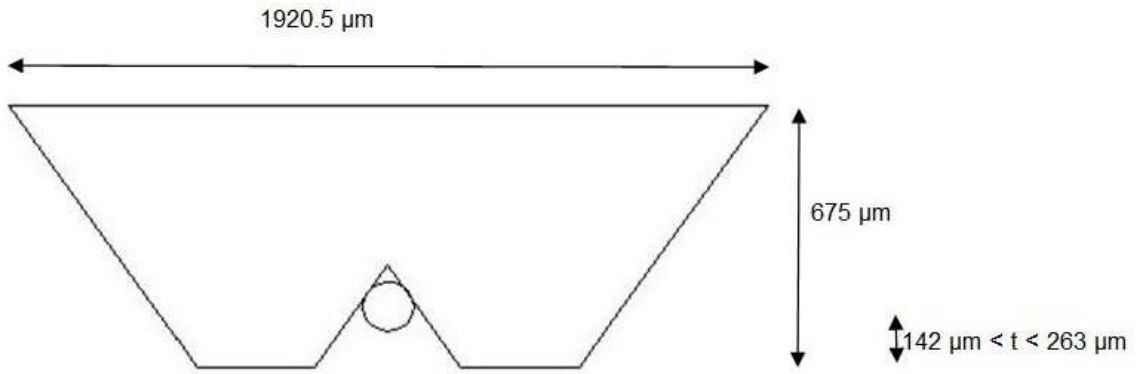

Figure 4.2.3: The schematic diagram of the V-groove to fit the optical fiber (before thinning)

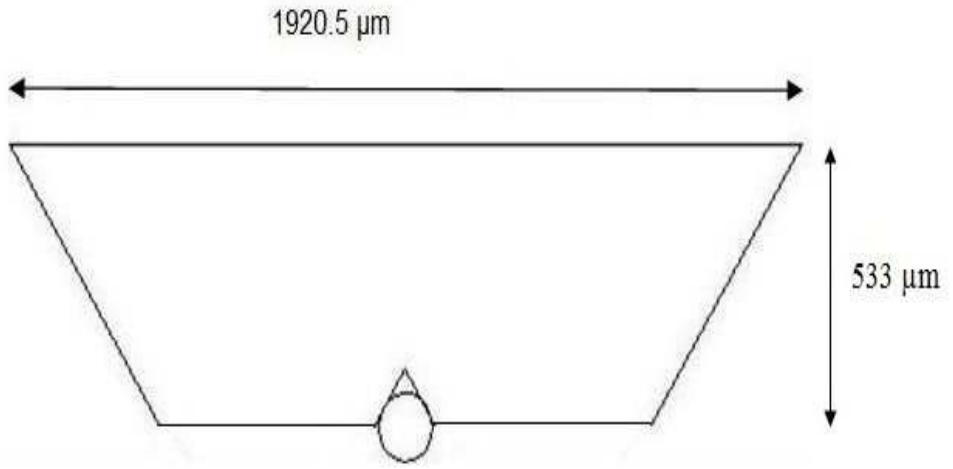

Figure 4.2.4: The schematic diagram of the V-groove to fit the optical fiber (after thinning)

Ragavendra Shankar Murthi has contributed a lot for developing the sanding process.

The arrangement of the sample chip is shown below in Figure 4.2.5.

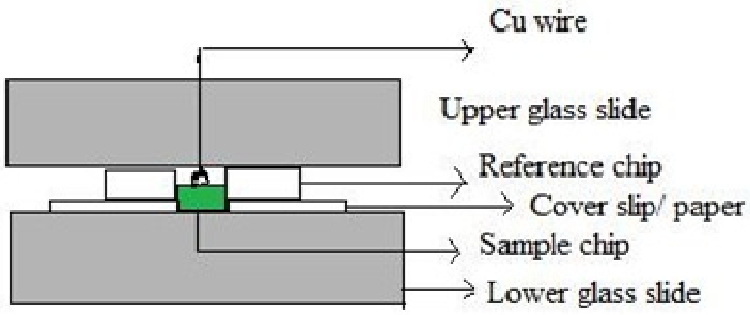

Figure 4.2.5 (a): The cross-sectional view of sanding arrangement (first step)

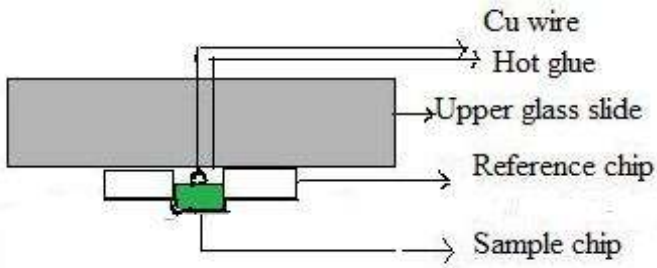

Figure 4.2.5 (b): The cross-sectional view of sanding arrangement (second step)

At first, a glass slide is taken, the sample chip was placed upside down on the glass slide. Then two pieces of papers or cover slips are placed beside the sample chip. Afterwards, two reference Si chips were put on the cover slips. This paper or cover slip created the height difference between the reference chip and sample chip. A thin Cu wire (without insulation) was placed on the sample chip to keep the sample chip at right place. Then another glass slide was attached on the top of the whole arrangement with hot glue. Finally, the upper glass slide holds the sample chip and the reference chips with a difference of height with the reference chips. A Sanding machine (4'' *36'' Belt and 6'' Disc Sander) was used for thinning of chip. A wood-based holder is made to carry the glass slide. This holder contains two opposing magnets. In Figure

4.2.6, the holder is shown. Magnet one (the magnet with the hinge) carries the glass slide/ sample chip and magnet two (the fixed magnet) opposes the magnet one towards the sanding paper. Therefore, the sample chip was at tight contact with the sand paper for this opposing force. As the chip was at tight contact with the sand paper, so the sanding process was uniform and in-plane. For the mounting process, the glass slide was placed at tight contact with the sand paper, after that hot glue is applied on the other side, thereafter the hinge structure is attached with the glass slide. By following this procedure, the sample chip was placed at perfectly flat position on the sand paper. Therefore, the sample chip got equal sanding everywhere on its plane. The sanding was applied on the lager area (100 times larger) reference chip 100 times faster than the sample chip. So, the sanding on the sample chip can be precisely controlled.

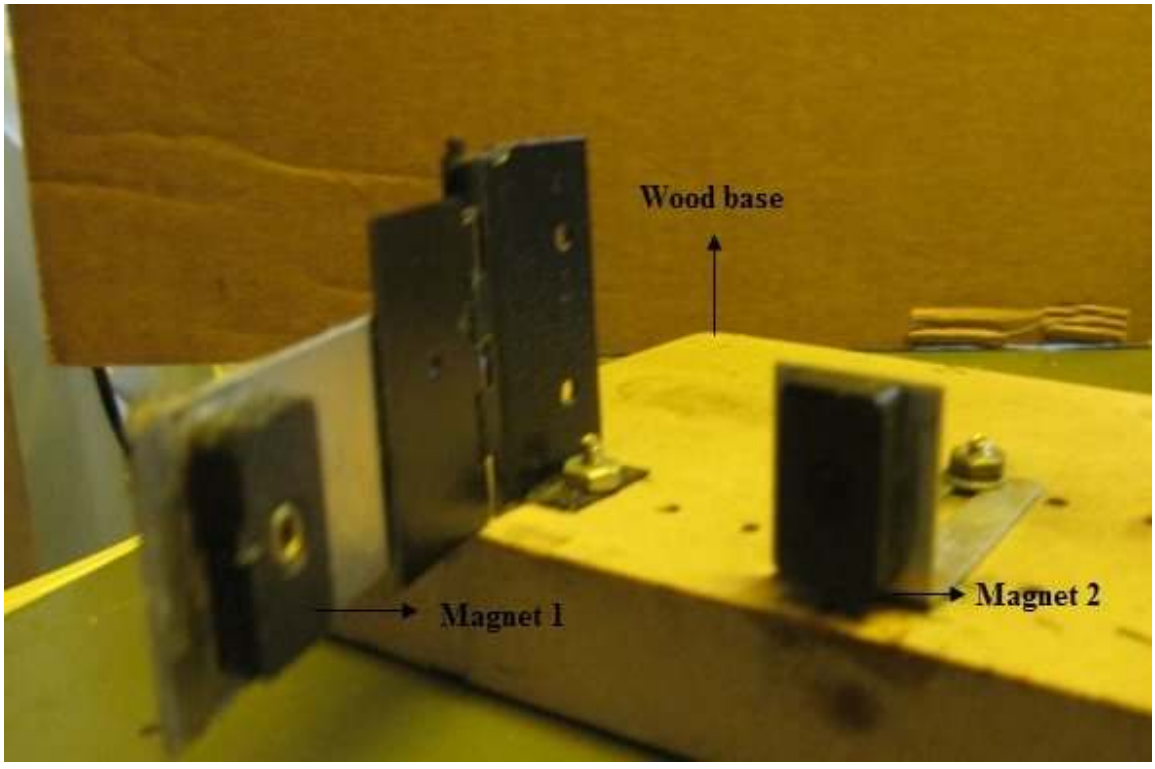

Figure 4.2.6 : The wood-based holder to carry the sample chip

In figure 4.2.7, it is shown that how the magnet one is at tight contact with the sand paper. A thousand grain sand paper was used for sanding.

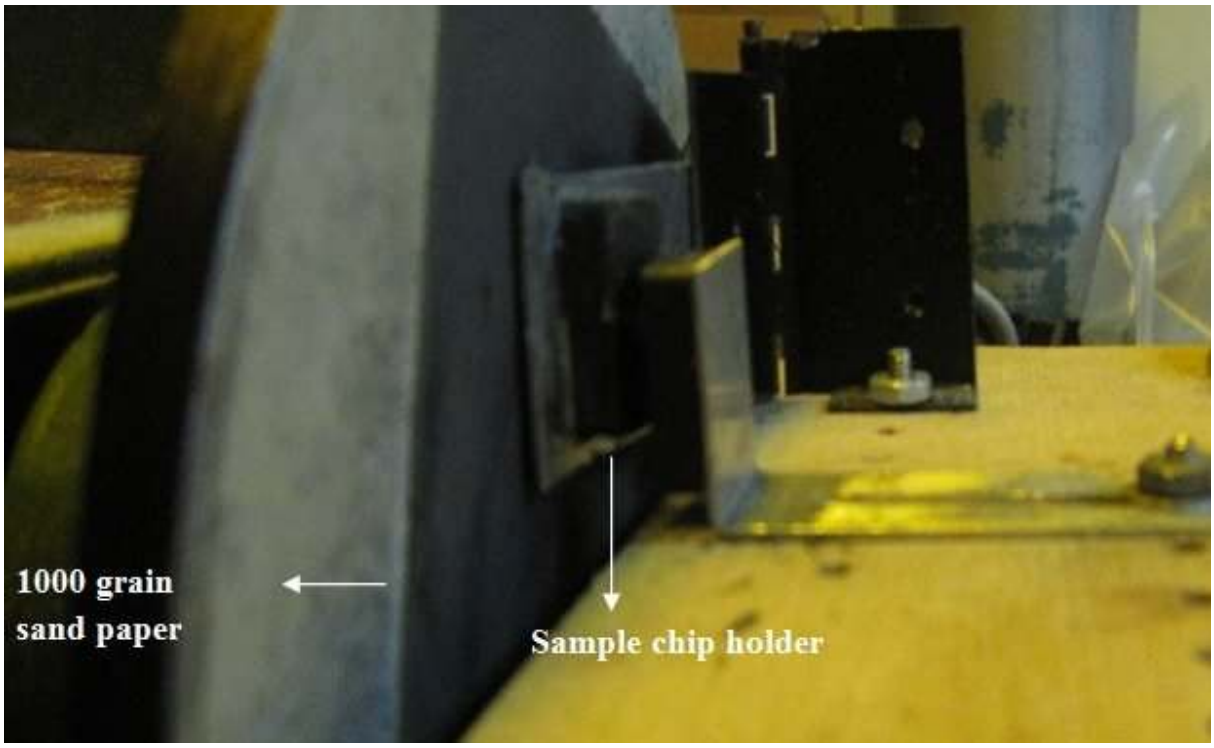

Figure 4.2.7: The thinning of sample chip arrangement

If the sample chip is at the same level after the sanding process, that means the thickness is reduced by the thickness of cover slip or paper. After the sanding process, the four edges of the reference pieces were checked under the microscope to see if they were in the same plane. By scrutinizing the depth of focus under microscope, a decision can be made on the leveling of the chip. By analyzing some experimental data, it can be stated that the thickness from 142 μm to 263 μm can be reduced from the sample chip with this sanding process. Therefore, a precise control over reducing thickness of Si chip in micrometer range had been accomplished with this experiment.

4.3 Preparing the Optical Fiber

This project used a 125 μm diameter fiber designed to support a single mode at a wavelength of 0.633 microns. Its core was about 3 microns in diameter, and the entire fiber was coated with a 50 micron thick coating, bringing its total diameter to 225 microns. This outer coating was stripped by the Micro-Strip precision stripper. Then a light scratch was made on the cladding of the fiber with a diamond scriber. Only a very little pressure is needed, and too much will crush the fiber. A light, single pass of the scribe should produce a scratch that is invisible to the naked eye. By carefully grasping both ends of the fiber and applying a gentle tension, the ends were pulled apart. Then both tips at the ends of the fiber were checked under the microscope. Both ends of the fiber should be of high quality without any trace of breaking. As the light rays are guided through the fiber to the lens, so the ends of the fiber need to be perfect. Also, the refractive index of the fiber is matched with the lens and epoxy.

4.4 Assembly Process

4.4.1 The Assembly of the Probe

The first step in the assembly process is to attach the fiber to the sample chip. This process is done on a Teflon slab. Teflon is chosen because it is non-adhesive to epoxy. The 60 minutes epoxy is applied in the groove in the chip and then the chip is placed on the fiber. The length of the extended fiber is determined under the microscope. The requirement for the length of the extended fiber is 150 μm. The chip slides along the fiber until 150 μm protrudes. The sliding of the chip is done with micropositioner. This process is a self-aligned process. As the fiber fits in the V-groove, the chip will move smoothly along the fiber. In figure 4.4.1.1, the chip with the extended fiber is shown. Here, the fiber fits in the groove perfectly.

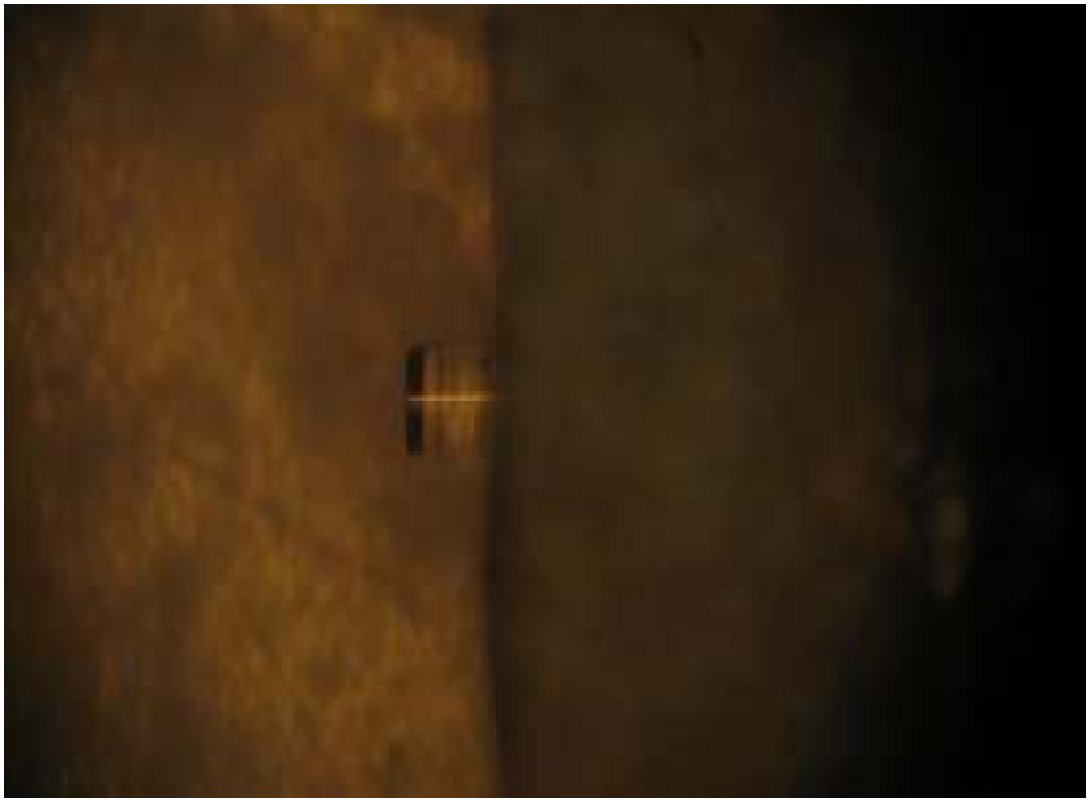

Figure 4.4.1.1: The enlarged view of the chip and the fiber. The fiber is extended by 150 μm

The second step is to attach the GRIN lens to the fiber-chip assembly. A 2 mm inner diameter Teflon tube is used for the assembling process. The top half of the Teflon tube is removed to observe the process. First the lens is placed inside the tube, then the 60 minutes epoxy and then the extended fiber tip. The joint between the lens and the fiber is very fragile. So, it should be handled very carefully. The refractive index of the epoxy is well-matched to the refractive index of the lens and fiber to pass the light rays with minimal reflections.

The third step is to place the lens-fiber-chip arrangement into the 2 mm diameter stainless steel probe. If the assembly fits well in the probe, the components are in the same plane and in line. In Figure 4.4.1.2, the completed construction is shown.

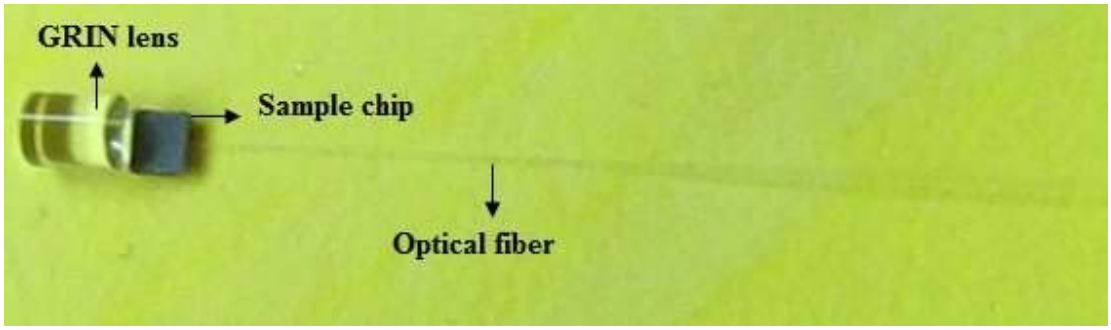

Figure 4.4.1.2: The completed construction of the lens, fiber and the chip

4.4.2 The Optical Arrangement

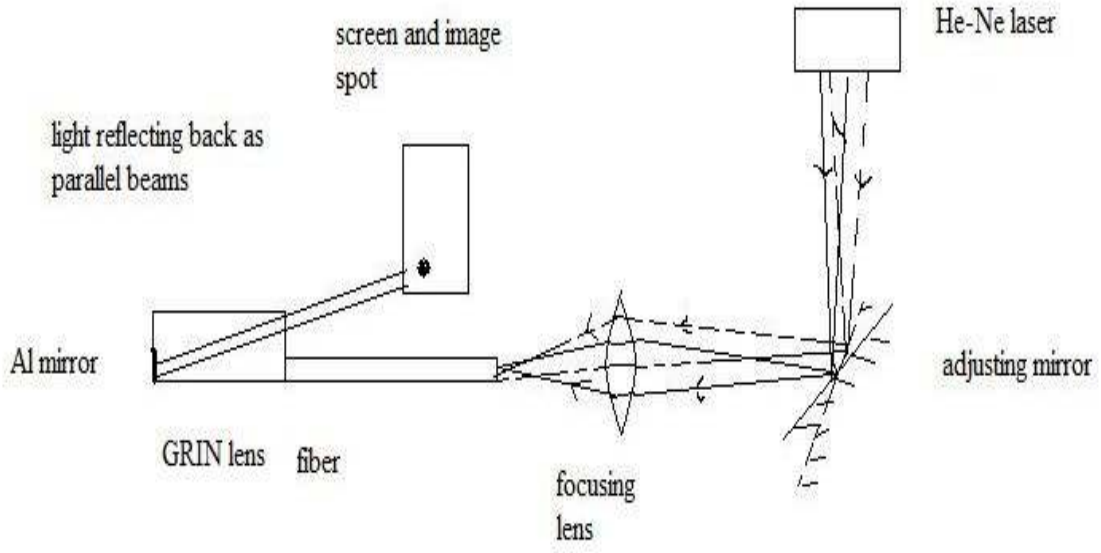

Figure 4.4.2.1: The schematic diagram of the optical arrangement

The optical arrangement consists of a He-Ne laser at a wavelength of 0.633 μm, an adjustable

mirror, a lens and an optical stage. The light ray spreads from the source, then it is reflected by the mirror, then it goes through a lens to achieve a focused image at the tip of the fiber. The components of the optical arrangement are shown in Figure 4.4.2.1. The mirror is placed after the source to adjust the axis of the light, adding flexibility to the system. The lens is focuses the light at the end of the fiber. The spot size should be 2.6 μm at the fiber tip. The NA of the fiber and the lens have to be matched for optical propagation of light through the core. If the NA of the lens is larger than the NA of the fiber, the spot will be less than 2.6 μm. Then the light would not propagate effectively through the fiber. If the NA of the lens is much smaller than the NA of the fiber, then the spot size will be larger than 2.6 μm, and much of the light would not enter the core. The figure 4.4.2.1 illustrates the NA matching of the fiber and lens. It is known that A= sinΘ, so the angle of the light rays of the lens has to be same to the angle of the light rays of the fiber. We place the end of the fiber at the focus of the lens, for an NA of 0.12, the focused spot size is 2.6 μm.

The probe was placed on an optical stage. This optical stage can be shifted in three directions, along the x, y and z axes. Centering the 2.6 μm core on the focused spot is very difficult.
The NA of the lens depends on the distance between the laser source and lens. In addition,
The light must enter along the axis of the fiber. By shifting the adjusting mirror, the axis of light can be matched. The dotted line in Figure 4.4.2.1 illustrates the off-axis light rays, and the dark line shows the on-axis light rays that are matched to enter to the core of the fiber.

We can adjust the mirror and we can search three ways to get the light through the core. By adjusting the mirror, we tried to be on the right axis to the fiber. Then by shifting the microscope objective in X, Y and Z direction, the core of the fiber can be found. If the light

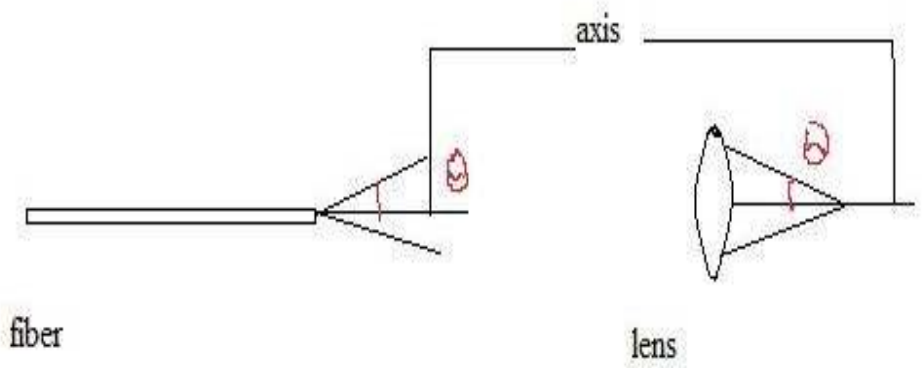

Figure 4.4.2.2: NA matching of fiber and lens

goes through the core, then a very bright spot (high intensity light) is observed on the image screen. If the stage is shifted by 3 μm, then a drastic change of the bright spot is observed, and that means the light is no more through the core. So, if the light is going through the core, a very small change of 3 μm makes the fiber to cross the diameter of the core and hence produces a blurry image spot (low intensity light). Again, if the light is going through the cladding the image spot does not change drastically for the shifting of the microscope objective. Because the diameter of the cladding is 125 μm and it produces the same blurry image spot within this diameter range. So, by looking at the image spot a decision can be made whether the light is going through the core or cladding. Also another determining point is that when a very small change in shifting of microscope objective changes the image spot from bright to blurry drastically.

In figure 4.4.2.3, it is shown that the NA of the lens is matched with the NA of the fiber. The

light is focused at the tip of the fiber and all light is going through the core.

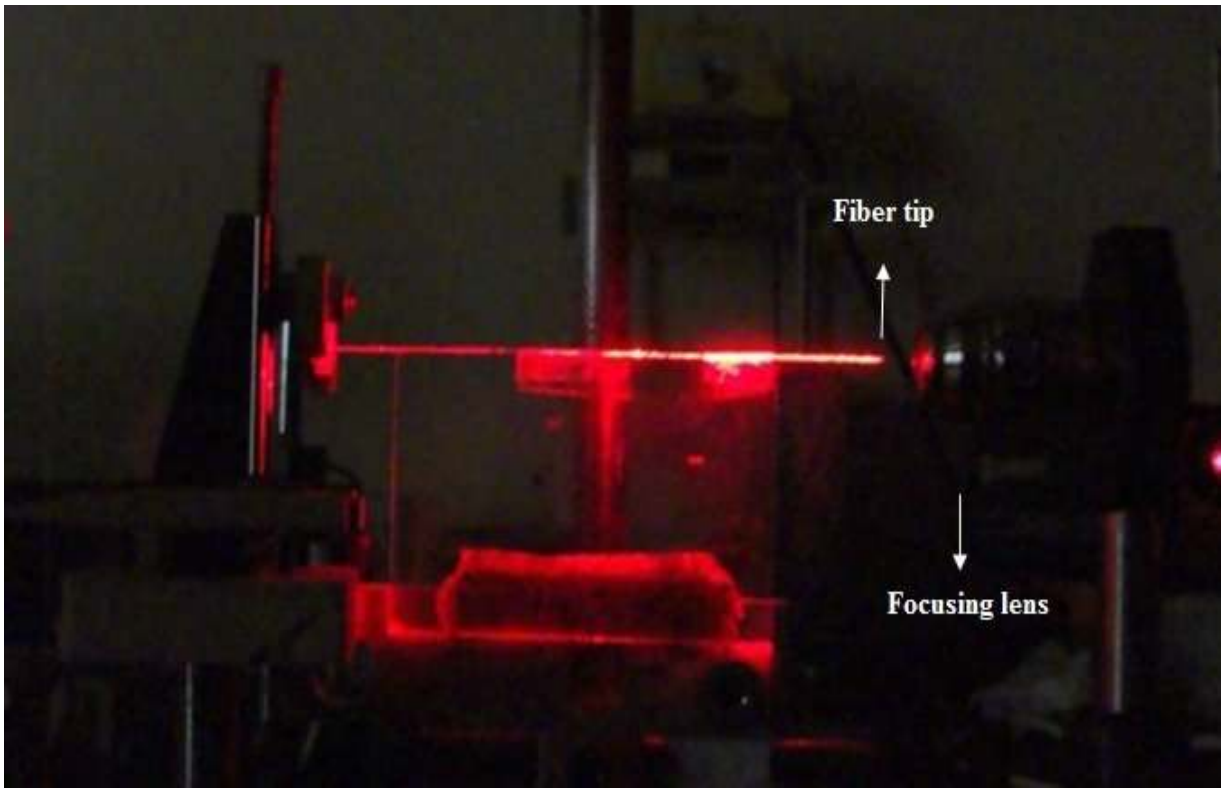

Figure 4.4.2.3: The optical arrangement with visible laser source

The numerical aperture (NA) of the optics is set by the NA of the optical fiber which is 0.12. The next step is to inspect how the light is reflected from the mirror of the GRIN lens. The design of the probe requires that the light should reflect back from the mirror of the GRIN lens to the scanning mirror of the MEMS chip. It is observed that when light hits the mirror of the GRIN lens, the light reflects back as a parallel beam, and no light passes through the other side. As we choose $\pi/8$ lens for the design, light should come back as a parallel beam. The light makes two passes through the lens, that means the oscillation is $\pi/4$,

and still it should come out as parallel beam according to lens specification. Therefore, the theory of the propagation of light through the GRIN lens is checked, shown in Figure 4.4.2.1. The angle of the reflected light is important. If light reflects at too large an angle it may not hit the scanning mirror. By measuring the reflecting angle of three sample probes, we found that the range of the angle is 10 to 15 degree which is acceptable. This precise angle range validates how accurately the fiber was mounted with the lens. In figure 4.4.2.5, the measurement is shown. Here, $\Theta = \tan^{-1}(a/b)$

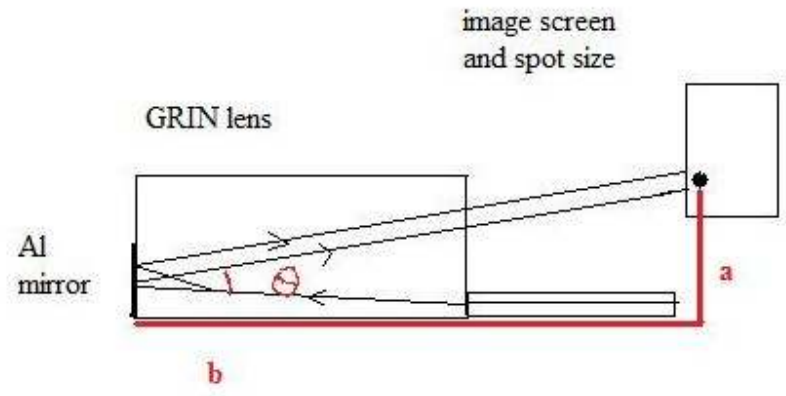

Figure 4.4.2.5: Measurement of reflecting angle

The optics related to the fiber and the GRIN lens was tested and a satisfactory result was obtained. As the final MEMS chip is not available, the scanning mirror characteristics cannot be tested. But by doing this experiment, practical experience with the path of the light rays is obtained. This experience will be useful to work with the real MEMS chip.

CHAPTER 5

RESULTS AND DISCUSSION

To summarize, a procedure for thinning the chip has been demonstrated, a procedure for assembling the components has been established. Moreover, the optics relating the fiber and the GRIN lens have been tested. We were able to get the light through the core of the fiber and observed that the light reflected back from the mirror of the GRIN lens. The reflecting angle of the rays were also accurate to hit the scanning mirror.

All the experiments have been done with sample chips, because the real MEMS chips re not ready yet for testing. After getting the real MEMS chips, some experiments will be set to test the scan range, response time, linearity, repeatability, resolution, working distance and flatness of field. We would like to quote the required parameters from the original proposal [11]:

1. Scan range: He-Ne laser light will be coming out as parallel beam on the mirror while the scanning control signal is applied to it. The scan range will be calculated from the range of reflected light on the position sensitive detector (PSD). The acceptable scan range is not less than 14 degree.

2. Response time: The signal from the PSD will be compared to the scan control signal to measure the response time. The acceptable response time is shorter than 1 msec.

3. Linearity: The linearity will be calculated from the plot of beam location on the PSD vs. control voltage. The acceptable non-linearity is less than 10%.

4. Repeatability: The repeatability will be evaluated by measurements made on test gratings. The acceptable repeatability is less than 0.1 pixel.

As described previously the resolution and depth of focus depend on the choice of numerical aperture. The optical system will be evaluated by measurements made on test gratings.

1. Resolution: An acceptable resolution will be about 2.6 microns.
2. Working distance: An acceptable working distance will be 50 to 400 microns.
3. Flatness of field: An acceptable flatness of field will be less than 40 microns.

The focused spot will be projected on a screen, and video images will be obtained with a frame grabber and analyzed off line. Preliminary tests will be performed in visible laser light at 0.633 μm, followed by more extensive tests at the operating wavelength of 1.3 μm. As a final check, one-dimensional images of resolution test patterns will be obtained.

In future the tests that are mentioned above will be done. The final step of this project is to integrate and test the OCT endoscope in vivo. This part will be done at the University of Arizona with their existing test equipment.

CHAPTER 6

CONCLUSIONS

The objective of this thesis is to develop the techniques needed to implement a miniaturized, forward-looking endoscope. In addition, some experiments were conducted to learn about the practical obstacles. To get a strong joint between the fiber and the lens was one of the challenges. Another challenge was to get the light through the core and test the characteristics of the GRIN lens. We developed a standard assembly procedure and an effective optical arrangement for the probe. The process is developed with 2 mm diameter probe In the future, 1 mm diameter probe will be developed.

A future part of this project is to implement the probe in an in-vivo set-up. This test will be performed at the University of Arizona. The success of the study will be assessed based on: 1) the ability to successfully introduce the endoscope into the stomach of 12 rats, 2) the ability to image at least one-half of the area of the gastric wall, and 3) the ability to measure the thickness of the mucosa, submucosa and total stomach wall thickness within the limits of comparison of histological sections and *in vivo* tissue (correlation better than 0.7) [11]. By analyzing data of the animals, the endoscope will ultimately be available for human studies.

BIBLIOGRAPHY

[1] Huang D, Swanson EA, Lin CP, Schuman JS, Stinson WG, Chang W, Hee MR, Flotte T, Gregory K, Puliafito CA. "Optical coherence tomography," Science 1991:254:1178-81.

[2]http://www.globalspec.com/LearnMore/Optics_Optical_Components/Optical_Components/GRIN_Lenses

[3] Wu J, Conry M, Gu C, Wang F, Yaqoob Z, Yang C. "Paired-angle-rotation scanning optical coherence tomography forward-imaging probe," Optics Lett 2006:31(9):1265-7.

[4] Pan Y, Li Z, Xie T, Chu CR. "Hand-held arthroscopic optical coherence tomography for in vivo high-resolution imaging of articular cartilage," J. Biomed. Optics 2003 Oct.:8(4):648-54.

[5] Piyawattanametha W, Fan L, Hsu H, Fujino M, Wu MC, Herz PR, Aguirre AD, Chen Y, Fujimoto JG. "Two-dimensional endoscopic MEMS scanner for high resolution optical coherence tomography," Conference on Lasers and Electro-Optics (CLEO) 2004.

[6] Yeow JTW, Yang VXD, Chahwan A, Gordon ML, Qi B, Vitkin IA, Wilson BC, Goldenburg AA. "Micromachined 2-D scanner for 3-D optical coherence tomography," Sensors and Actuators 2005:A117:331-40.

[7] Chong C, Isamoto A, Toshiyoshi, H. "Optically modulated MEMS scanning endoscope," IEEE Photon. Technol. Lett. 2006:81(1):133-5.

[8] Jung W, McCormick DT, Zhang J, Wang L, Tien NC, Chen Z. "Three-dimensional endoscopic optical coherence tomography by use of a two-axis microelectromechanical scanning mirror," Appl. Phys. Lett. 2006:88(16):163901.

[9] Xie T, Xie H, Fedder GK, Pan Y. "Endoscopic optical coherence tomography with new MEMS mirror," Electronics Letter 2003 Oct.:39(21):1535-6.

[10] http://www.nsgamerica.com/index.php?lang=english&page=grin_andselfoc

[11] Dr.Martin Feldman, Dr. Dooyoung Hah, Dr. Jennifer Barton. Optical probe for microscopic cancer identification in minute structures", the research proposal, 2008.

[12] MEMSCAP, Inc., http://www.memsrus.com/documents/PolyMUMPs.flow.show.pps.

[13] Lih-Yuan Lin, Evan L. Goldstein, Robert W. Tkach."On the Expandability of Free Space Micromachined Optical Cross Connects", Journal Of Lightwave Technology, Vol.18, No. 4, April 2000

VITA

Anandi Kalyan Dutta was born and raised in Bangladesh. She received her Bachelor of Science in Electrical and Electronic Engineering from American International University-Bangladesh, in 2006. She enrolled to Louisiana State University to pursue her graduate studies in August, 2009. She is currently a candidate for the degree of Master of Science in Electrical Engineering, which will be conferred in December, 2010.